USGS
science for a changing world

Using Remotely Sensed Data to Map Joshua Tree Distributions at Naval Air Weapons Station China Lake, California, 2018

Scientific Investigations Report 2020–5053

U.S. Department of the Interior
U.S. Geological Survey

Cover Photo. Joshua tree (*Yucca brevifolia*) photographed on Bureau of Land Management lands—Coolgardie Mesa near the Naval Air Weapons Station China Lake, San Bernardino County, California. Photographed May 7, 2020, by Todd C. Esque, U.S. Geological Survey.

Using Remotely Sensed Data to Map Joshua Tree Distributions at Naval Air Weapons Station China Lake, California, 2018

By Todd C. Esque, Patrick E. Baird, Felicia C. Chen, David Housman, and J. Tom Holton

Scientific Investigations Report 2020–5053

U.S. Department of the Interior
U.S. Geological Survey

U.S. Department of the Interior
DAVID BERNHARDT, Secretary

U.S. Geological Survey
James F. Reilly II, Director

U.S. Geological Survey, Reston, Virginia: 2020

Suggested citation:
Esque, T.C., Baird, P.E., Chen, F.C., Housman, D., and Holton, J.T., 2020, Using remotely sensed data to map Joshua Tree distributions at Naval Air Weapons Station China Lake, California, 2018: U.S. Geological Survey Scientific Investigations Report 2020–5053, 13 p., https://doi.org/10.3133/sir20205053.

ISSN 2328-0328 (online)

Acknowledgments

We thank Brandon Barr and Lisa Vanamburg—Natural Resources Specialists, Desert Integrated Products Team, Naval Facilities Engineering Command Southwest—for providing financial and logistical support, and manuscript review. Daniel J. Leavitt, Ph.D., and Cynthia Hopkins of Naval Air Weapons Station China Lake (NAWS–CL), contributed substantial time and effort ensuring we had safe access to remote sites at NAWS–CL, providing relevant background to the work, and reviewing this manuscript. Bill Linsdale safely guided us through NAWS–CL backcountry. We thank B. Gottsacker, A. McDonald, G. Olson, and J. Swart for assisting in remotely surveying more than 4,500 km^2 of habitat for Joshua trees. This work was funded through the Department of the Navy, Military Interdepartmental Purchase Request N47609-17-MP-001XY.

Contents

Figures

Tables

Conversion Factors

International System of Units to U.S. customary units

Multiply	By	To obtain
	Length	
meter (m)	3.281	foot (ft)
kilometer (km)	0.6214	mile (mi)
	Area	
square kilometer (km^2)	247.1	acre
square kilometer (km^2)	0.3861	square mile (mi^2)

U.S. customary units to International System of Units

Multiply	By	To obtain
	Length	
foot (ft)	0.3048	meter (m)

Datum

Horizontal coordinate information is referenced to the North American Datum of 1983 (NAD 83).

Abbreviations

AUC	area under the curve
CHM	Canopy Height Model
FINTC	Fort Irwin National Training Center
lidar	light detection and ranging
NAWS–CL	Naval Air Weapons Station China Lake
SDM	species distribution model
USFWS	U.S. Fish and Wildlife Service
USGS	U.S. Geological Survey
UTM	Universal Transverse Mercator

Using Remotely Sensed Data to Map Joshua Tree Distributions at Naval Air Weapons Station China Lake, California, 2018

By Todd C. Esque,[1] Patrick E. Baird,[1] Felicia C. Chen,[1] David Housman,[1] and J. Tom Holton[2]

Abstract

Species distribution models (SDMs) that are derived through inference have been used to provide important insights toward species distributions. Their inferences can be robust in relation to known presences, but SDMs have error rates that cannot be quantified with certainty. For large plant species with unique signatures and in sparsely vegetated habitats, object-oriented satellite image interpretation provides a useful alternative to the more commonly used SDM approach. We tested visual image interpretation techniques in a pilot project to map the distribution of the Joshua tree (*Yucca brevifolia*), an arborescent succulent plant endemic to the Mojave Desert of North America. Naval Air Weapons Station China Lake (NAWS–CL) required assistance in mapping the distribution of Joshua trees across the 4,715 square kilometer (km^2) military installation in support of their national security mission. Joshua trees were present on 1,307 1-km^2 cells in the species distribution model, or 27.7 percent of the military installation. This increases the published range of Joshua trees at NAWS–CL by 90 percent and corrects for two stands of Joshua trees that were previously identified but do not exist. Remotely sensed satellite data in combination with ground surveys of Joshua trees produced a more accurate distribution map at a 1-kilometer resolution than did previous SDMs based on correlative modeling (area under the curve [AUC] 0.9064 versus 0.5848, respectively). Ancillary comparison with light detection and ranging (lidar) data indicated that satellite and lidar data were equally successful with slightly different sources of error, but that using them in combination produced the best results.

Introduction

Accurate species distribution information is fundamental to (1) evaluating species' distributional changes in response to habit disturbances and other environmental variation and (2) determining conservation status for conservation planning and resource management activities (Guisan and Thuiller, 2005; Elith and Leathwick, 2009). Species distribution modeling (SDM) can be biased by the location and number of presence points available for modeling, while lacking absence data. Such biases may reduce SDM accuracy in areas with restricted access. Object-based image interpretation using remotely sensed data is a feasible alternative to SDM and is capable of producing more accurate maps in cases where large focal subjects with unique characteristics occur in open vegetation types. One such plant is the Joshua tree (*Yucca brevifolia*).

The Joshua tree is a slow-growing arborescent succulent in the Asparagaceae family (Angiosperm Phylogeny Group III, 2009; Chase and others, 2009), in a subgroup commonly known as yuccas. It is endemic to the Mojave Desert of the southwestern United States, at elevations ranging from 700 to 2,100 meters (m) in California, Nevada, Utah, and Arizona (Rowlands, 1978). Joshua tree populations are at risk from wildfires associated with invasive grasses (Loik and others, 2000; DeFalco and others, 2010) and from climate change (Barrows and Murphy-Mariscal, 2012). Joshua tree recruitment is episodic and dependent on an array of favorable environmental conditions; thus, changes in climate that lead to less precipitation and higher temperatures could be detrimental to Joshua trees (Reynolds and others, 2012).

[1]U.S. Geological Survey.

[2]Department of Defense.

This study encompasses the Department of Defense, Naval Air Weapons Station China Lake (NAWS–CL), near Ridgecrest, San Bernardino County, California, United States of America. Habitat enhancement and the protection of native plant communities and the native wildlife (including any Federally listed species) that depend on these communities is an integral part of NAWS–CL's natural resources ecosystem management strategy detailed in the installation's Integrated Natural Resources Management Plan (Tierra Data, Inc., 2014). Areas of dense Joshua tree woodland are identified as a sensitive habitat warranting special consideration in land-use planning.

Ground-based mapping of Joshua trees at NAWS–CL is challenging because of limited road access, the distribution of high security areas that are off-limits to non-essential personnel, and the presence of unexploded ordnance in backcountry areas. Because of restricted access, fewer species occurrence records are available from this and most other large military installations in the desert southwest, potentially reducing the accuracy of species distribution models within these areas. Therefore, we developed a cost-effective remote sensing technique using publicly accessible satellite imagery—Google Earth Pro. This technique was of sufficient resolution to plan for future demographic surveys and was not hampered by access constraints. We used a combination of object-oriented analyses in three stages: (1) reviewing satellite imagery; (2) conducting ground surveys to validate remotely sensed results; and (3) conducting subsequent inspection of satellite imagery using the combination of previous satellite imagery analysis, ground surveys, and a small sample of light detection and ranging (lidar) data provided to us by the Department of Defense, Fort Irwin National Training Center.

The objective for this study was to conduct Joshua tree distribution mapping as a baseline to establish a statistically rigorous sampling protocol toward determining the status of Joshua tree populations at NAWS–CL. The results of this study are important to determine current species status and to establish a baseline for monitoring future trends in Joshua tree populations. The success of this study will determine potential future uses of the technology toward a rangewide distribution map for Joshua trees.

Methods

Study Area

The study area encompasses the entirety of NAWS–CL with up to a 1-kilometer (km) buffer outside the boundary and covers 4,715 square kilometers (km^2) of desert basin and range habitat (fig. 1). Elevation ranges from 448 m in the Panamint Valley to 2,695 m at the summit of Maturango Peak in the Argus Range.

Publicly available Google Earth satellite imagery was used exclusively to create a provisional map of Joshua tree distributions prior to ground truthing the data on NAWS–CL at a 1-km^2 resolution. To conduct the survey, the Fishnet toolbox in ArcMap 10.5 was used to create a grid of 4,715 1-km^2 cells that covered the entire NAWS–CL facility, which consists of a North Range and a South Range (fig. 1). The grid was compatible with the global Universal Transverse Mercator (UTM) coordinate system. Cells inside and intersecting the boundary of the installation were visually inspected in satellite imagery for the presence or absence of adult Joshua trees at a standardized eye elevation of 150–300 m for initial surveys. The eye elevation (the altitude above the land surface provided to the user as a view of the scene in the imagery) that was used provided a view of each cell with sufficient resolution to perform a thorough survey of each cell by scanning systematically from the northwest corner along the northern boundary and following around the perimeter of the cell, then placing the scanning window in the northwest corner and moving diagonally to the southeast corner, and likewise placing the scanning window in the southwest corner and moving to the northeast corner to complete the scan with 100 percent coverage (fig. 2). Satellite imagery survey was limited to adult Joshua trees because their branches are easily recognizable in medium to high quality satellite imagery (fig. 3), especially where other large yucca species such as *Yucca schidigera* are absent. By contrast, single stem Joshua trees are difficult or impossible to distinguish from shrubs, trees (pinyon pines and junipers—*Pinus* spp. and *Juniperus* spp., respectively), or other yucca species. Areas that were difficult to search owing to variability of imagery quality sometimes required varying the eye elevation or using different time frames within the historical satellite imagery (from time frame including 2013 to 2017 in the North Range and only 2014 in the South Range because of poor image quality in years prior to 2014), providing higher resolution or better contrast than more recent imagery.

A team of six biologists inspected a total of 4,979 1-km^2 cells. Each observer inspected 830 cells. To calculate observational error, 264 cells (5.6 percent of all cells) were inspected separately by different observers. Visual scans of each cell were targeted as 2-minute time intervals to standardize the work and maintain cost effectiveness. If no Joshua trees were identified within the allotted time, then the cell was designated as an absent cell. Observers denoted whether Joshua trees were present or absent in each cell by placing waypoints, either at the location of an identified Joshua tree for a present cell or near the cell center for an absent cell (fig. 4).

Error and Error Reduction

Field visits to NAWS–CL were conducted to validate and correct the remotely sensed results. This activity was limited by road and hiking access because of base restrictions for

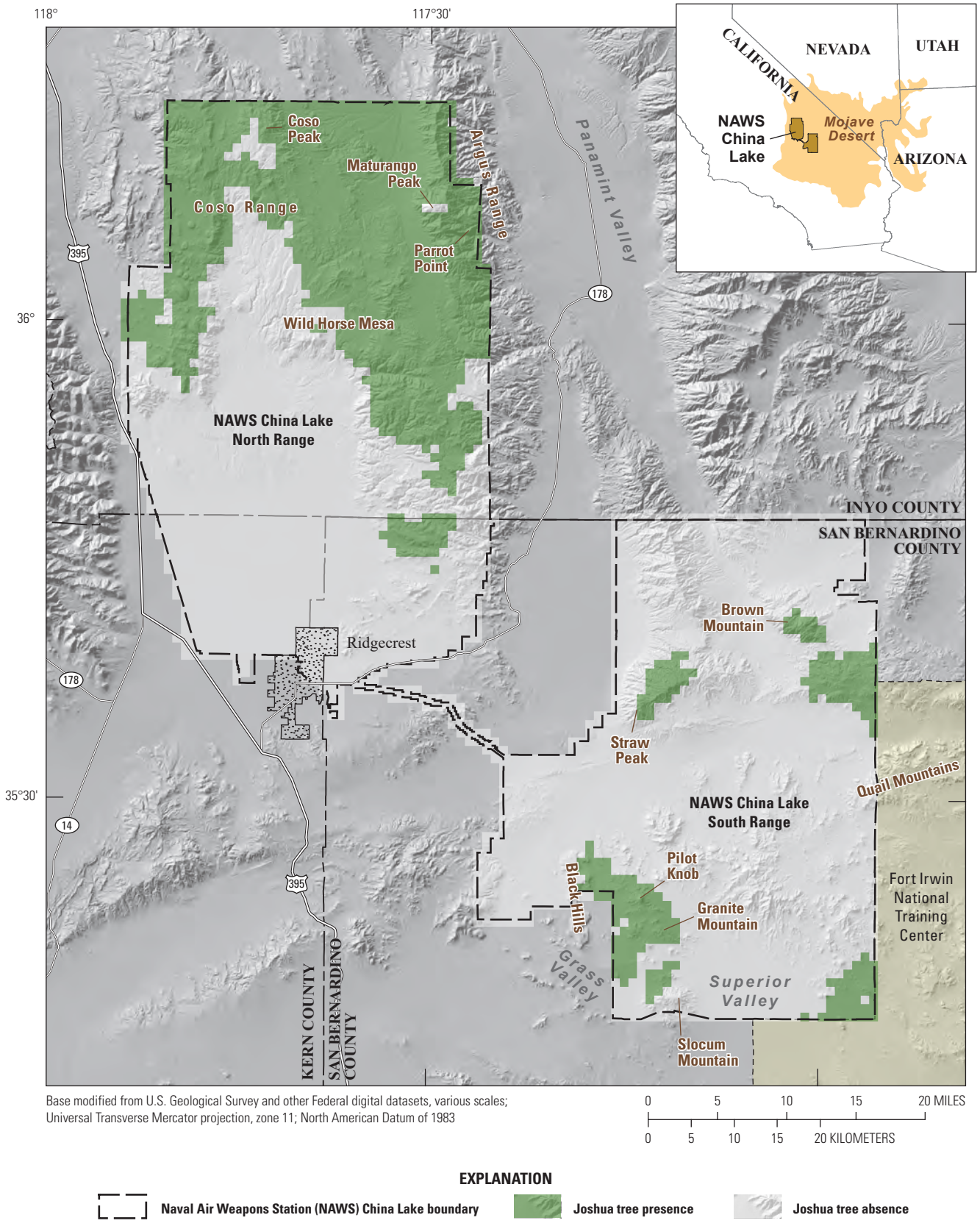

Figure 1. Naval Air Weapons Station China Lake, California, study area for determining the distribution of Joshua trees at 1-square-kilometer (km^2) resolution in 2018.

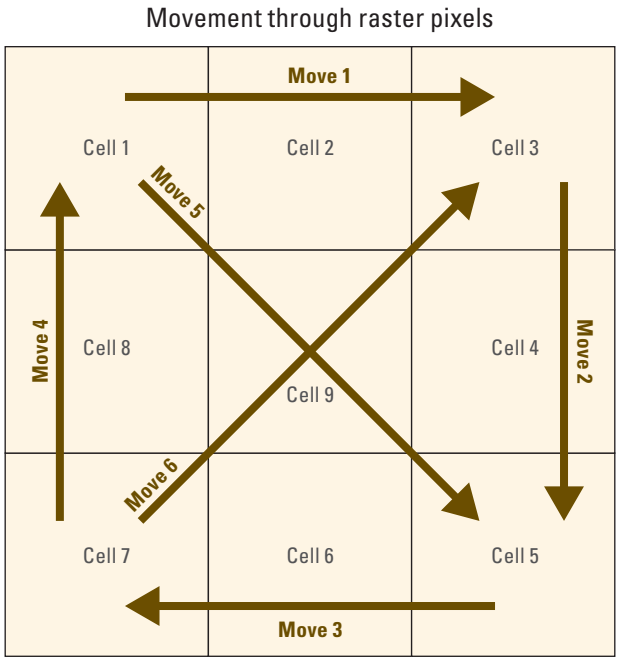

Figure 2. Scanning technique used to determine presence or absence of Joshua trees at Naval Air Weapons Station China Lake, California, in 2018 on 1-square-kilometer (km^2) survey areas. (1) The scanning view is moved eastward across the top of the cell to the northeast boundary of the cell; (2) then scanned southward to the southeast corner; (3) westward to the southwest corner; and (4) northward, back to the northwest corner. Next, (5) the scanning window is placed in the northwest corner and moved diagonally across the cell to the southeast corner and (6) finally placed in the southwest corner and shifted diagonally to the northeast corner to complete the coverage.

security and safety. We visited 256 random points along the access roads of NAWS–CL with binoculars, and each was no closer than 500 m from the next. In addition to the 256 sites that were randomly selected for inspection, we also evaluated an additional 315 cells that were intersected during our travels among the sites. All these data were used to evaluate errors. At each point, the compass bearings and distances to the nearest Joshua trees were recorded. For each cell that was driven through, regardless of containing random points, Joshua tree presence or absence within view of the road was noted. Special care was taken to note the location of any trees found in cells identified as absent during the satellite imagery inspection, and vice versa—the absences of trees in cells that had been identified as present were also recorded.

To further reduce error in the development of the Joshua tree distribution map, we prioritized field surveys for cells that were difficult to evaluate during satellite imagery inspections, thus having increased potential for error (fig. 4). Such areas included the edges of the Joshua tree stands, isolated cells that were designated with presence in otherwise large expanses of absence, cells with conflicting results identified by multiple observers, and cells that simply had poor imagery quality. We predicted that Joshua trees on the edges of stands would be more difficult to locate in satellite imagery than those in areas of dense Joshua tree presence or absence. To test this, we focused on areas that transitioned between Joshua tree absence and presence according to the provisional map. The results of field surveys were used to correct and validate the provisional map. The increased experience in interpreting remotely sensed data with field validation improved our ability to make additional changes to cell status (presence versus absence) by what we termed as informed inspection on the provisional map—subsequent to field validation. If a change of status was required based on the informed inspection, then it was termed an informed correction.

Informed corrections were performed using satellite imagery in cells suspected of being incorrect for any of the reasons mentioned above but where visitation was not possible during the field surveys because of distance from roads or safety or security restrictions. For absence cells that were adjacent to presence cells, we inspected the areas where presence was noted, and if we felt confident that we had previously identified Joshua trees correctly, we followed topographical and geological features (for example, unique soil texture visible in the image) from where trees were found into adjacent cells where Joshua trees were previously undetected. The waypoints created in the database by the original observer were inspected and either confirmed by the informed inspection or discarded as erroneous. A complete record for all cells was maintained and archived. All individual presence cells that were isolated by absence cells were reconsidered using informed inspection and corrected as necessary. Thus, the final Joshua tree map is the result of the initial satellite imagery survey that was reinforced by two additional phases of corrections: field validation and informed inspections of imagery in areas that were otherwise inaccessible owing to large distances from roads or mission safety related site access restrictions.

Model Comparison

The final distribution map that was created for this report was compared to currently used models of Joshua tree distributions for this region, including Rowlands, 1978; Cole and others, 2003; and Godsoe and others, 2008, to determine differences in the amount of Joshua habitat between this model and the others. Area under the curve (AUC) statistics were used to compare data from ground-truthed cells (total number = 571) with the data collected from satellite data versus the same cells from a recently published Joshua tree habitat map (Godsoe and others, 2009). We compared the remotely sensed model of Joshua tree distribution and a previously published SDM model of Joshua tree distribution

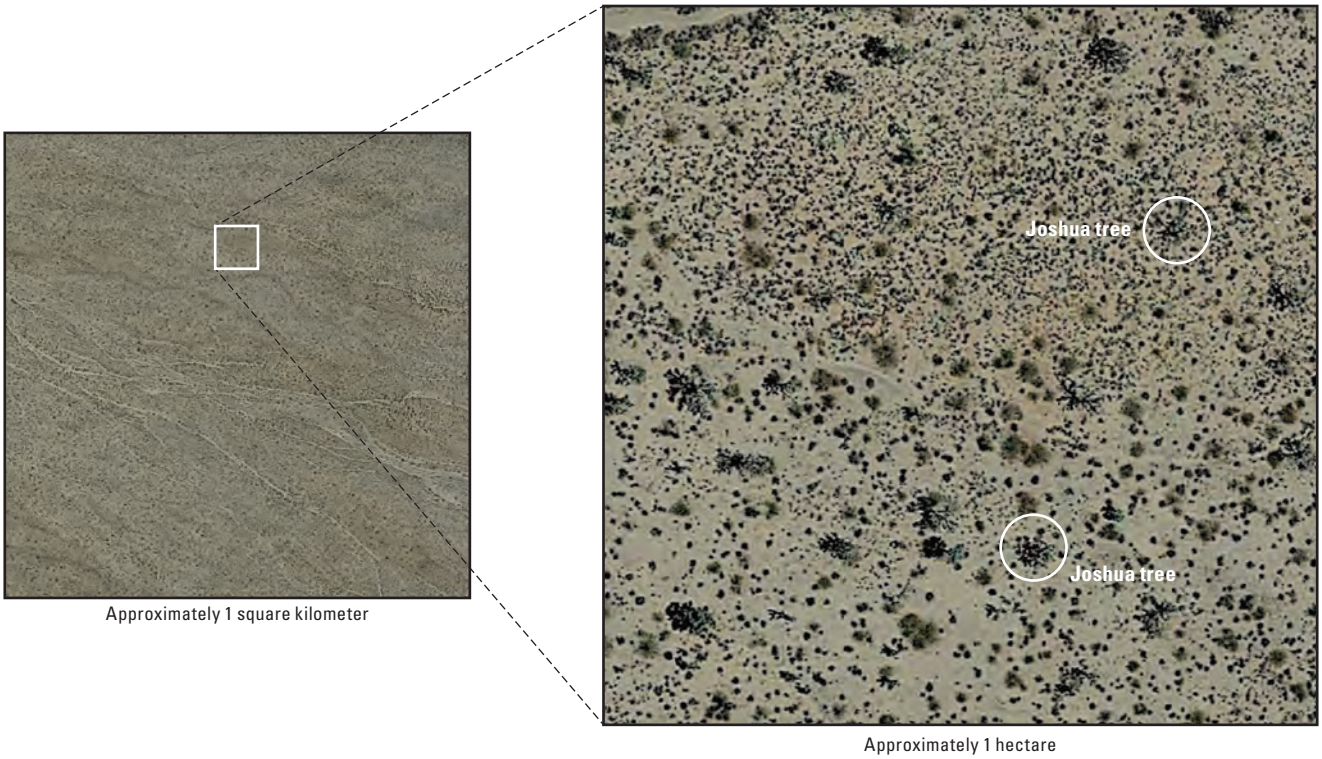

Figure 3. Scalar views used to determine presence/absence of Joshua trees in Google Earth Pro at Naval Air Weapons Station China Lake, California. The large square on the left is a 1-square-kilometer (km^2) grid square that was used to identify search areas. Visual inspection of a focal area (for example, the small white square) of potential Joshua tree habitat at 1,600-meter eye altitude. Note two examples of adult Joshua trees in the view at this resolution are circled.

(Godsoe and others, 2009) with 571 ground-based validation sites of Joshua tree distribution using AUC statistics (Hanley and McNeil, 1982; Fielding and Bell, 1997).

Use of Lidar to Detect Joshua Trees

Performed concurrently but separately from this study, the neighboring Department of Defense, U.S. Army–Fort Irwin National Training Center (FINTC) conducted successful experiments to identify Joshua trees using lidar. This lidar database overlapped with small areas of NAWS–CL that coincided with the detailed ground surveys.

Fusion Version 3.6 (McGaughey, 2018) was used for lidar processing, and ArcMap 10.5 was used for final data scrubbing of lidar outputs to identify Joshua trees ≥12 feet tall within the FINTC and some areas in adjacent NAWS–CL. The Fusion software package developed by the U.S. Forest Service was used to create a Normalized Canopy Height Model (CHM) discussed in the Fusion manual (McGaughey, 2018, p. 29). A Normalized CHM creates a high-resolution raster to determine the height of objects above ground. This was based on the distance from the Earth's surface to the top of the object (EarthDefine, 2016). All final shapefile outputs were inspected and cleaned manually to remove false identifications such as rock outcrops, *Populus fremontii* (cottonwood) trees, and man-made structures.

The following set of programs within Fusion were executed to determine *Yucca brevifolia* point locations and heights. The program GroundFilter was used to filter out all bare-earth points used to create the bare-earth model. These bare-earth points within each land analysis system (LAS) tile were used to create the bare-earth model with GridSurfaceCreate, which was used to normalize the CHM. CanopyModel was then used to generate the Normalized CHM from the lidar point cloud. A watershed algorithm called TreeSeg was then applied to the normalized CHM to generate basins to create local minima that represented the dominant clumps of trees, or in this case, individual *Yucca brevifolia* (McGaughey, 2018, p. 143). The Integrate geoprocessing tool was also used in ArcMap 10.5 to clean up point locations that were identifying the same trees that were within 10 m of each other. All outputs were projected to WGS 1984 UTM Zone 11N, which was the original projection of the LAS files.

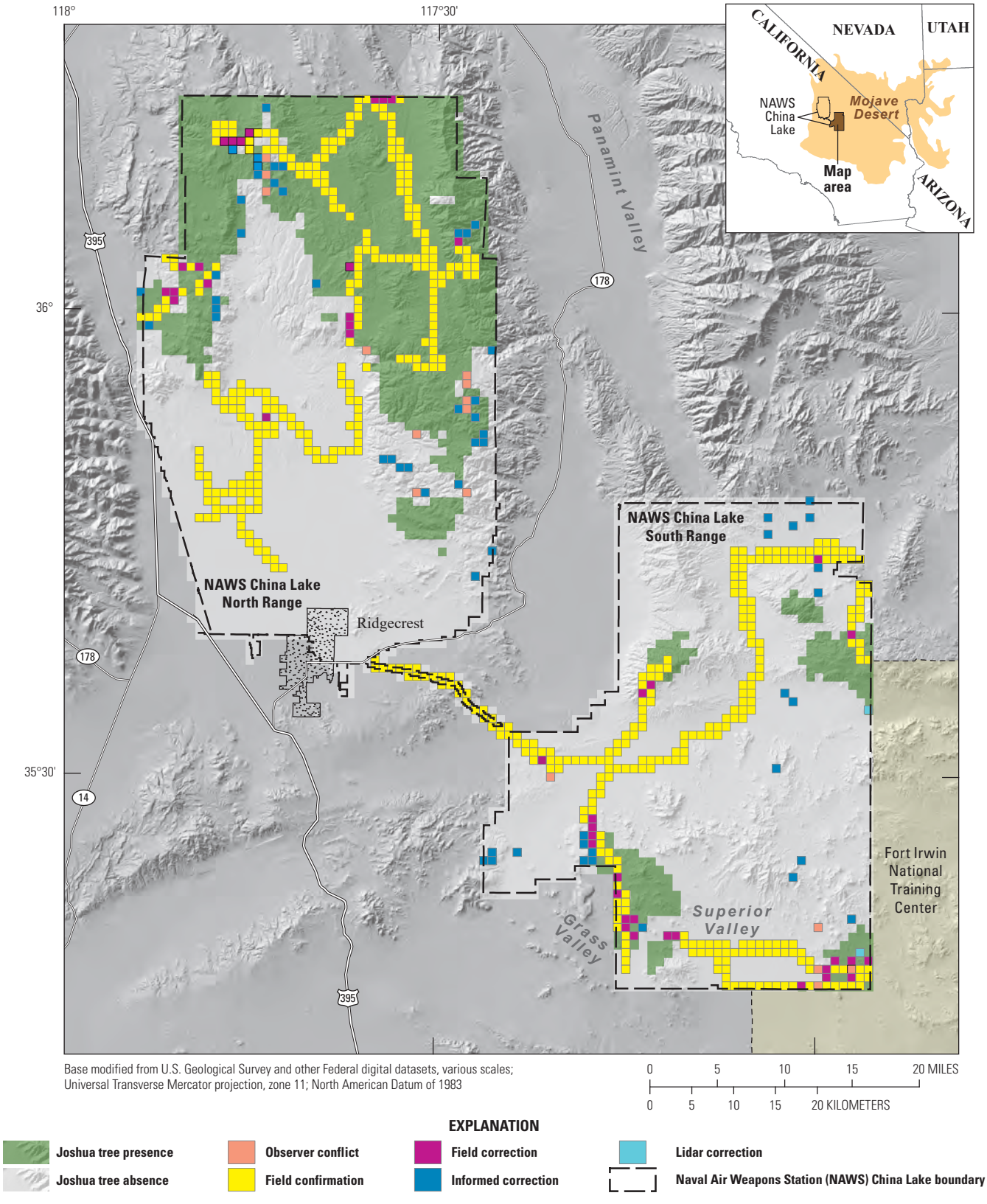

Figure 4. Error analysis of Joshua tree distributions at Naval Air Weapons Station China Lake, California. Colors represent areas where the determination of presence (green areas) or absence (light gray areas within the military boundary) were changed based on field surveys (yellow areas), informed corrections (blue areas), or more recently acquired light detection and ranging (lidar) data (turquoise areas). Field surveys resulting in a change of plot status are the magenta areas.

Results

Descriptions of Joshua Tree Presence

All 4,715 1-km² cells within the boundaries of NAWS–CL were evaluated. The final map product shows that 27.7 percent (1,307 cells) of the naval installation is currently occupied by Joshua trees (table 1). Joshua trees are present on 39.4 percent of the North Range (1,029 of 2,612 cells) and cover only 13.2 percent of the South Range (278 of 2,103 cells). The elevational range of Joshua trees across all of NAWS–CL is from 764 to 2,450 m (2,468 to 7,916 feet [ft]). The median elevation at which Joshua trees occur differs between North and South Ranges; the median elevation at which Joshua trees are present in the North Range is 1,726 m (5,576 ft), whereas Joshua trees grow at a median 1,192 m (3,851 ft) in the South Range. The overall elevation of South Range is lower than the North Range, with the highest point of the South Range only reaching 1,638 m. The southwestern foothill region of the Argus Mountain Range on the North Range is the lowest elevational area where Joshua trees were located (764 m; table 1).

Distributions in the North Range

In the North Range, there is one large nearly continuous population of Joshua trees covering 1,045 km², occurring between 1,025 and 2,450 m above sea level in the vicinity of the southwestern foothills of the Argus Range and Parrot Point, respectively (fig. 5). Joshua trees cover most of the Argus and Coso Ranges except small areas at the highest elevations of Maturango and Coso Peaks. However, the map indicates Joshua tree occupancy of the grid sections containing these peaks because lower elevations areas within the 1 km² are occupied by Joshua trees. Field surveys found Joshua trees intermixed in pinyon/juniper habitats at elevations as high as 2,450 m. It is possible that Joshua trees are present in low densities above the stated elevational maximum but could not be identified using satellite imagery and were inaccessible during field surveys. The southern edge of this population is delimited by steep south- and southwest-facing slopes of Wild Horse Mesa and the southeast facing slopes of the Coso Range. The northern, eastern, and western edges of this population continue beyond the boundaries of NAWS–CL but were not surveyed. A smaller population of Joshua trees covering 36 km² is present between 764 and 1,192 m elevation in the far southwest foothills of the Argus Range. This population is only separated by a 2-km gap from the larger stand previously described. It is possible that Joshua trees are present in the cells between the two populations but were not identified in satellite imagery. Alternatively, it is possible that Joshua trees are unable to occupy the steep, rocky south-facing slope as it drops 400 m in elevation between the two populations.

Distributions in the South Range

The South Range of NAWS–CL contains six distinct populations of Joshua trees that range in size from 11 to 83 km² (fig. 6). The largest population occupies areas on and surrounding the Black Hills, Pilot Knob, and Granite Mountain, extending westward into Grass Valley and beyond the NAWS–CL boundary where it thins out and was not surveyed further. This population occupies an elevational range of 871 to 1,456 m. A second population occupies the northwest part of Slocum Mountain between 1,112 and 1,239 m in elevation covering 11 km² and is only separated from the Granite Mountain population by a narrow unnamed valley. Three of the South Range populations are restricted to high elevational areas: Straw Peak, Brown Mountain, and the Quail Mountains. The Straw Peak population covers 28 km², with an elevation range from 1,154 to 1,638 m and is completely contained within the boundaries of NAWS–CL. The Brown Mountain population covers 13 km², ranges from 1,141 to 1,511 m in elevation, and exists entirely within the boundary of NAWS–CL. The Quail Mountains population is the second largest, occupying 54 km². This population extends east into the FINTC and was not surveyed via satellite or field past the boundary of NAWS–CL. The Quail Mountains and Brown Mountain populations are only separated by 1 km and may be a continuous population that remains unsubstantiated. The last population present in the South Range is in the southeasternmost corner of the NAWS–CL. This stand covers 38 km² and has the smallest Joshua tree elevational range, 927 to 1,074 m. The population extends both south and east into the FINTC and was not surveyed beyond the boundaries of NAWS–CL. This population stands out as the only one that occupies entirely flat habitat in lower elevational terrain.

Table 1. Results of Joshua tree presence and absence during mapping surveys across the range of the Naval Air Weapons Station China Lake (NAWS–CL), California, in 2018.

NAWS–CL ranges	Total number cells surveyed	Number of cells Joshua tree absence	Number of cells Joshua tree presence	Joshua tree presence as percentage
Both Ranges	4,715	3,408	1,307	27.7%
North Range	2,612	1,583	1,029	39.4%
South Range	2,103	1,825	278	13.2%

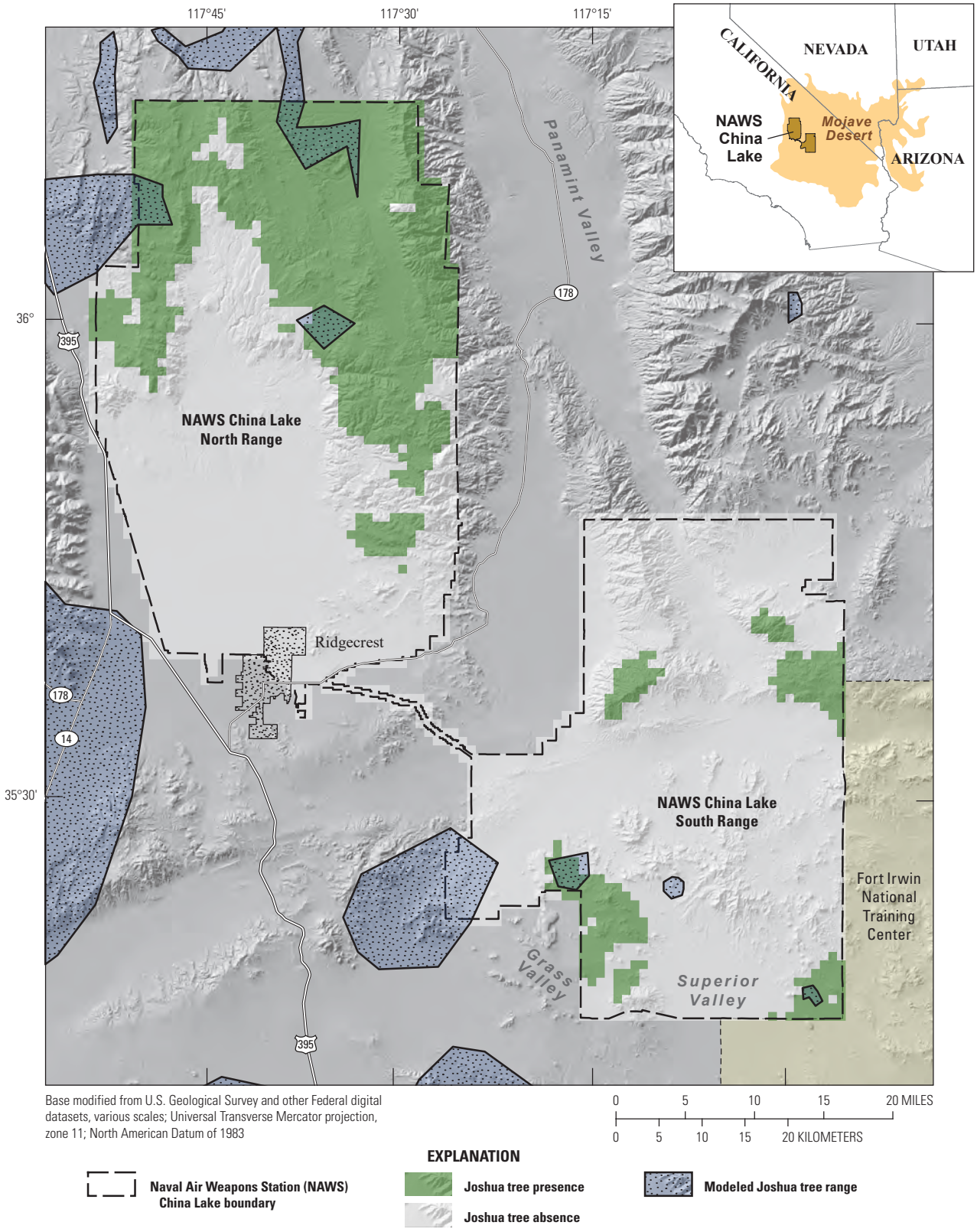

Figure 5. Final Joshua tree distribution map at Naval Air Weapons Station China Lake, California, in comparison with a previous distribution model (Godsoe and others, 2008). The dark green areas represent Joshua tree presence, and the light gray areas (within the military boundary) represent Joshua tree absence according to the present document. In contrast, the overlaid blue-gray pixelated areas represent Joshua tree presence, and all other areas within the military boundary, but without blue-gray pixelated patterns indicate Joshua tree absence according to Godsoe and others (2008).

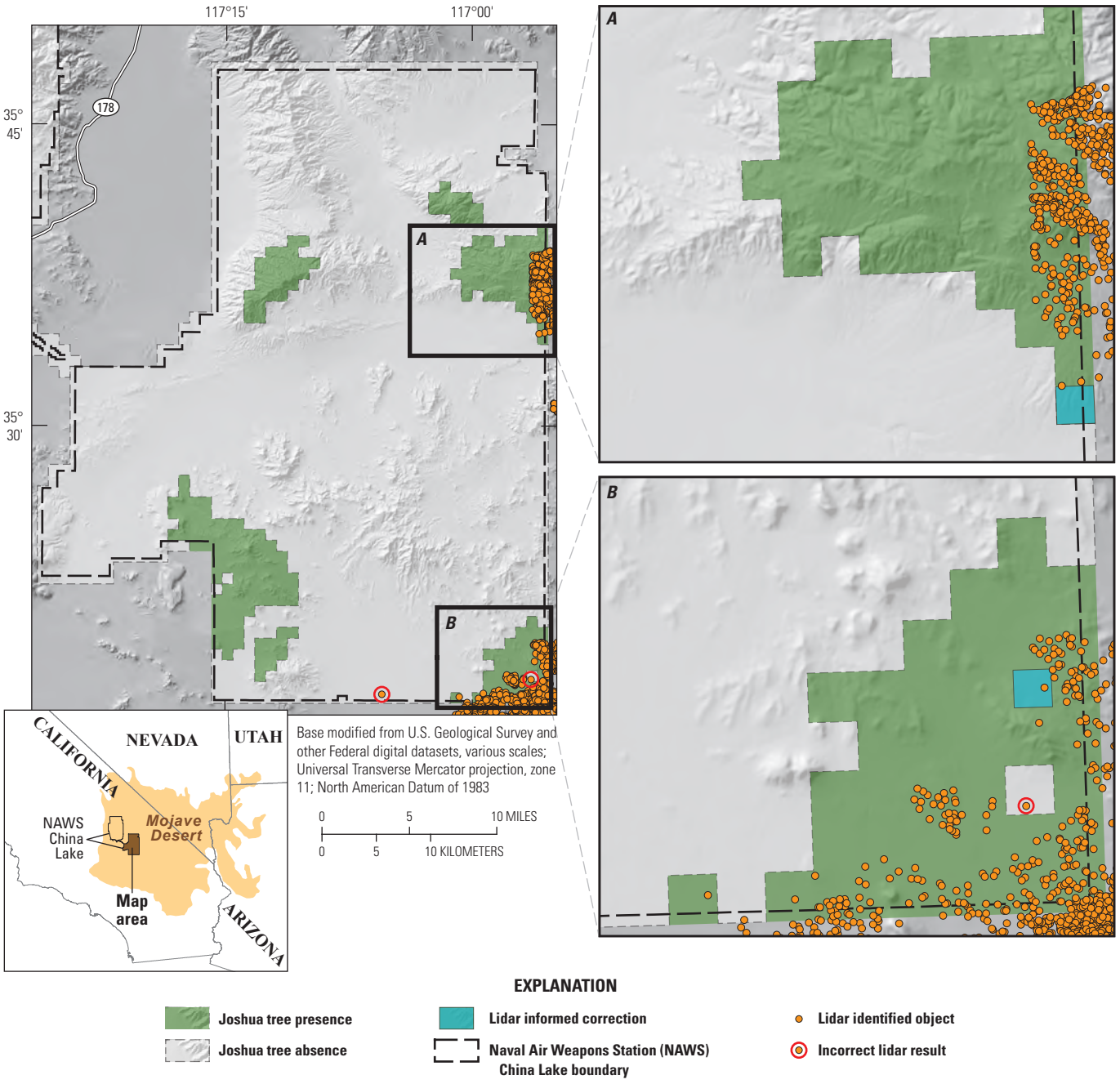

Figure 6. Comparison of Joshua tree distributions using satellite images versus draft Joshua tree distributions derived from light detection and ranging (lidar) data at Naval Air Weapons Station China Lake, California, 2018.

Comparison Among Models

Ground-based validation survey data for the presence/absence of Joshua trees (N = 571 cells) were compared to the remotely sensed survey of Joshua trees and with a recently published SDM model (Godsoe and others, 2009) of Joshua tree distribution in the same 571 cells. The remotely sensed model had an AUC of 0.0964 with a point biserial correlation of 0.8456. The published SDM model did not perform as well, with an AUC of 0.5848 with a point biserial correlation of 0.3323.

Sources and Management of Error

There were 264 cells inspected by two different observers to quantify observer error in the satellite imagery survey. Observers only had differing results in 15 (5.7 percent) of the

cells checked for error. Of those, the correct classification for three cells was determined during field surveys, and the correct classification for the remaining 12 cells was made as a result of informed inspections of the satellite imagery because they were not accessible on the ground. All 15 of the cells with conflicting initial survey results had low Joshua tree presence. Error can also be quantified as the number of cells that changed from the original satellite imagery survey to the final map product. Cells were corrected either based on field observations or by an informed inspection of the satellite imagery (table 1). Field survey inspection covered 571 cells, 528 of which were determined to have been correctly identified during the satellite imagery survey. The 43 misidentified cells (7.5 percent error) were corrected as a result of field surveys, and 40 of the 43 field corrections changed a previously absent cell to a presence cell. As hypothesized, those that were corrected were often located on the edge of a Joshua tree population, and those cells that were correctly identified often occurred either within the interior of a Joshua tree population or within large area of absences.

The informed inspection corrected 59 cells in total with 27 cells changed to presence and 32 cells converted to absence. Two cells were corrected based on lidar data provided by FINTC. During production of the final map, a total of 104 (2.2 percent) of all cells were corrected from the original provisional Joshua tree distribution map based solely on satellite imagery.

Cost

The remote sensing survey required approximately 157 hours of personnel time. Field surveys were performed with three employees over five 10-hour days, adding 150 work-hours. The informed inspection was performed on an estimated 400 cells with an average of 5 minutes spent in each cell, or a total of 33 work-hours. The cumulative time spent on this map product is estimated to be 340 work-hours.

Discussion

The current distribution of Joshua trees delineated in the new distribution map substantially increases the documented presence of Joshua trees at NAWS–CL. A comparison with previous Joshua tree distributions (Rowlands, 1978; Cole and others, 2003; Godsoe and others, 2008) indicates that the new distribution map increases the known presence of Joshua trees within the boundaries of NAWS–CL by 90.5 percent (fig. 5). The previously published distribution of Joshua trees for the North Range of NAWS–CL was characterized as three small distinctive stands of Joshua trees. By contrast, the revised map, presented here (fig. 5), indicates that all three of these stands are part of a contiguous population, and additionally, there are two small stands of limited distribution in the southern part of the North Range that were previously not identified. The South Range of NAWS–CL was previously characterized by four very small and disjunct stands of Joshua trees in the southern half of the range, the largest of which straddled the western boundary of the installation. The revised map substantially increases the areal extent of Joshua trees, which are now represented in all four quadrants of the South Range, albeit represented by less extensive stands than in the North Range. Additionally, we found no evidence of Joshua trees in two polygons of Joshua tree presence depicted in the previous distribution maps. However, the resolution of the remotely sensed data for those locations is of lower quality than most other areas at NAWS–CL; therefore, the potential for error in that region of the installation is greater. We attribute the improvement in the new distribution mapping over previous mapping and modeling efforts to the use of remotely sensed data as well as to increased access to the installation that we were provided. There is no evidence that previous mapping efforts had the benefit of site visits to the NAWS–CL facility (Rowlands, 1978; Cole and others, 2003; Godsoe and others, 2008).

Areas at the edge of dense Joshua tree stands were consistently the most difficult to classify from satellite imagery. This is likely because at higher elevations such areas are represented by smaller, younger growth forms of Joshua trees. Smaller, younger growth form Joshua trees are more difficult to detect in images that also have more well-developed vegetation communities of large plants such as junipers that can confound visual detection of similarly sized Joshua trees, and this illustrates one of the limitations to this method. This may explain why more cells were changed from absence to presence than vice versa. The three cells that were corrected to absence cells were isolated and contained structures or large creosote bushes that were previously misidentified for Joshua trees in the satellite imagery.

A combination of remotely sensed satellite data (for example, Google Earth) and lidar data with ground-truthing surveys appears to be ideal for identifying Joshua trees with the least error in landscapes. While we were remotely sensing Joshua trees, researchers at FINTC were simultaneously using lidar to detect and map Joshua trees. Lidar uses laser detection technology to identify the distribution of Joshua trees. From the sample of overlapping data, it appears that both lidar and the remote sensing technique were successful and had similar error values although with different sources of error. By ground truthing both lidar and satellite imagery in the field, we found that the lidar imagery improperly classified a dead deciduous tree as a Joshua tree and possibly a tall pole potentially placed during historical mining activities. The latter is inferred from the area that was traversed, but a pole was not actually observed. Conversely, some mapping cells that were up to 2 km from traveled routes had Joshua trees detected by lidar that were missed by initial remote sensing surveys and by ground searches. Furthermore, by using the

lidar data to review sites in satellite imagery, it was possible to locate and confirm individual Joshua trees that were previously undetected.

Another approach is to conduct species distribution modeling, which has been used extensively as a management and research tool to define sensitive habitats, identify previously unknown habitats, and direct searches for species (Graham and others, 2004; Elith and others, 2006). Species distribution modeling has been previously used in Joshua tree research as well (Godsoe and others, 2009; Smith and others, 2011; Cole and others, 2011; Barrows and Murphy-Mariscal, 2012). However, each of the previous uses of SDM for Joshua trees was to answer different questions than we addressed. The SDM method divides the landscape into many cells and then makes correlations between known presence/absence of a target species and environmental variables in each of the many cells. Then, using information about areas where presence/absence is not known, the modeling algorithm assigns the probability of the species of interest being present, based on the correlation with environmental values that are assigned to each cell. This requires large scale geographic correlational assignment of species presence. The new species distribution map based on object detection differs from SDM methods because the majority of presence/absence determinations were made by visual validation of presence either remotely, or in situ, or both. We propose that once an empirical map such as we developed at NAWS–CL is available for the range of Joshua trees, SDM can be used to provide greater insight into environmental relationships with Joshua tree distributions and demographic dynamics. The object-oriented remote sensing methods that we used on the Joshua tree distribution map for NAWS–CL are superior to the inferential distribution maps that can be created using SDM because the remotely sensed mapping product is based on empirical inspection of the habitat, thus accumulating fewer errors.

Manned or unmanned aircraft surveillance of habitats is a third alternative for mapping species distributions; this approach could potentially refine results from the previously described techniques. Although relatively straightforward to accomplish on public lands such as those administered by the Bureau of Land Management or the U.S. National Park Service, special planning may be required to secure access to sensitive sites at NAWS–CL and other such secure Federally administered lands. We propose that the use of lidar or near-remote sensing aircraft could be used to increase substantially the resolution of mapping adult Joshua trees.

It is important to note that the quality of the satellite images we used varied through space and time, influencing the accuracy of identifying Joshua trees consistently over large areas. Characteristics of the associated vegetation community may also influence the ability of observers to correctly identify Joshua trees. In locations where multiple arborescent yucca species co-occur (for example, *Y. schidigera* in parts of the east Mojave Desert), it may be particularly difficult to visually distinguish the different species of yucca. It is likely that such areas will require more extensive field and aerial surveys for ground truthing. In most cases, it will not be possible to detect Joshua trees that occur within the canopies of shrubs. Consequently, none of the currently available remote sensing methods are likely to facilitate demographic modeling completely because the smaller size classes of trees (that is, less than 1 m tall and possibly 30 years of age; Esque and others, 2015) will frequently not be visible from remotely sensed data of any type. However, it is possible that higher resolution surveillance methods such as lidar could be used to account for all but the shortest Joshua trees. For successful and complete demographic modeling, it will still be necessary for personnel to conduct ground-based demographic surveys.

Next Steps

The completion of the preliminary distribution map comes at a time when information about Joshua trees is of concern to management agencies across the Mojave Desert ecoregion. We found that the distribution of Joshua trees in a representative area of habitat could be successfully mapped using satellite imagery that is publicly available. Moreover, this technique provided a more accurate distribution map than was previously achieved using statistical modeling (SDM) approaches. Based on the results of this study, a consortium of academics, government researchers, and non-governmental agencies have proposed that similar methods be used to establish a rangewide map of Joshua tree distribution. At 4,715 km^2, NAWS–CL is approximately 3.4 percent of the entire Mojave Desert (for example, MacMahon and Wagner, 1985, estimate the Mojave Desert at 140,000 km^2) and likely constitutes 6 to 8 percent of the Joshua tree's entire range. The provisional distribution map required approximately 340 hours of work, suggesting that thousands more hours may be required to map the full distribution of Joshua trees in the Mojave Desert.

References Cited

Angiosperm Phylogeny Group III, 2009, An update of the Angiosperm Phylogeny Group (APG) classification for the orders and families of flowering plants—APG III: Botanical Journal of the Linnean Society, v. 161, no. 2, p. 105–121, https://doi.org/10.1111/j.1095-8339.2009.00996.x.

Barrows, C.W., and Murphy-Mariscal, M.L., 2012, Modeling impacts of climate change on Joshua trees at their southern boundary—How scale impacts predictions: Biological Conservation, v. 152, p. 29–36, https://doi.org/10.1016/j.biocon.2012.03.028.

Chase, M.W., Reveal, J.L., and Fay, M.F., 2009, A subfamilial classification for the expanded asparagalean families Amaryllidaceae, Asparagaceae and Xanthorrhoeaceae: Botanical Journal of the Linnean Society, v. 161, no. 2, p. 132–136, https://doi.org/10.1111/j.1095-8339.2009.00999.x.

Cole, K.L., Pohs, K., and Canella, J.A., 2003, Digital range map of Joshua tree (*Yucca brevifolia*): Corvallis, Oregon, U.S. Geological Survey, Forest and Rangeland Ecosystem Science Center, http://sagemap.wr.usgs.gov/ftp/regional/USGS/YUBRRangemap.shp.xml.

Cole, K., Ironside, K., Eischeid, J., Garfin, G., Duffy, P., and Toney, C., 2011, Past and ongoing shifts in Joshua tree distribution support future modeled range contraction: Ecological Applications, v. 21, no. 1, p. 137–149, https://doi.org/10.1890/09-1800.1.

DeFalco, L.A., Esque, T.C., Scoles-Sciulla, S.J., and Rodgers, J., 2010, Desert wildfire and severe drought diminish survivorship of the long-lived Joshua tree (*Yucca brevifolia*; Agavaceae): American Journal of Botany, v. 97, no. 2, p. 243–250, https://doi.org/10.3732/ajb.0900032.

EarthDefine, 2016, Spatial Cover Canopy Height Model (CHM): EarthDefine web page, accessed at www.earthdefine.com/spatialcover_chm/.

Elith, J., Graham, C.H., Anderson, R.P., Dudik, M., Ferrier, S., Guisan, A., Hijmans, R.J., Huettmann, F., Leathwick, J.R., Lehmann, A., Li, J., Lohmann, L.G., Loiselle, B.A., Manion, G., Moritz, C., Nakamura, M., Nakazawa, Y., Overton, J.M.M., Peterson, A.T., Phillips, S.J., Richardson, K., Scachetti-Pereira, R., Schapire, R.E., Soberón, J., Williams, S., Wisz, M.S., and Zimmermann, N.E., 2006, Novel methods improve prediction of species' distributions from occurrence data: Ecography, v. 29, no. 2, p. 129–151, https://doi.org/10.1111/j.2006.0906-7590.04596.x.

Elith, J., and Leathwick, J.R., 2009, Species distribution models—Ecological explanation and prediction across space and time: Annual Review of Ecology Evolution and Systematics, v. 40, no. 1, p. 677–697, https://doi.org/10.1146/annurev.ecolsys.110308.120159.

Esque, T.C., Medica, P.A., Shryock, D., DeFalco, L.A., Webb, R.H., and Hunter, R.B., 2015, Direct and indirect effects of environmental variability on growth and survivorship of pre-reproductive Joshua trees, *Yucca brevifolia* Engelm. (Agavaceae): American Journal of Botany, v. 102, no. 1, p. 85–91, https://doi.org/10.3732/ajb.1400257.

Fielding, A.H., and Bell, J.F., 1997, A review of methods for the assessment of prediction errors in conservation presence/absence models: Environmental Conservation, v. 24, no. 1, p. 38–49, https://doi.org/10.1017/S0376892997000088.

Godsoe, W.E., Strand, E., Smith, C.I., Yoder, J.B., Esque, T.C., and Pellmyr, O., 2009, Divergence in an obligate mutualism is not explained by divergent climatic factors: The New Phytologist, v. 183, no. 3, p. 589–599, https://doi.org/10.1111/j.1469-8137.2009.02942.x.

Godsoe, W.E., Yoder, J.B., Smith, C.I., and Pellmyr, O., 2008, Coevolution and divergence in the Joshua tree/yucca moth mutualism: American Naturalist, v. 171, no. 6, p. 816–823, https://doi.org/10.1086/587757.

Graham, C.H., Ferrier, S., Huettman, F., Moritz, C., and Peterson, A.T., 2004, New developments in museum-based informatics and applications in biodiversity analysis: Trends in Ecology & Evolution, v. 19, no. 9, p. 497–503, https://doi.org/10.1016/j.tree.2004.07.006.

Guisan, A., and Thuiller, W., 2005, Predicting species distribution—Offering more than simple habitat models: Ecology Letters, v. 8, no. 9, p. 993–1009, https://doi.org/10.1111/j.1461-0248.2005.00792.x.

Hanley, J.A., and McNeil, B.J., 1982, The meaning and use of the area under a receiver operating characteristics curve: Radiology, v. 143, no. 1, p. 29–36, https://doi.org/10.1148/radiology.143.1.7063747.

Inman, R.D., Esque, T.C., Nussear, K.E., Leitner, P., Matocq, M.D., Weisberg, P.J., Dilts, T.E., and Vandergast, A.G., 2013, Potential Habitat for the Mohave Ground Squirrel (*Xerospermophilus mohavensis*)—Is there room for all of us?: Endangered Species Research, v. 20, p. 1–18, https://doi.org/10.3354/esr00487.

Jones, T., and Goldrick, S., WildEarth Guardians, 2015, Petition to list the Joshua tree (*Yucca brevifolia*) under the Endangered Species Act, Petition submitted to the U.S. Secretary of the Interior Acting through the U.S. Fish and Wildlife Service: WildEarth Guardians, accessed May 23, 2018, at wildearthguardians.org.

Lenz, L.W., 2007, Reassessment of Y. brevifolia and recognition of Y. jaegeriana as a distinct species: Aliso, v. 24, no. 1, p. 97–104, https://doi.org/10.5642/aliso.20072401.07.

Loik, M.E., St. Onge, C.D., and Rodgers, J., 2000, Post-fire recruitment of *Yucca brevifolia* and Yucca schidigera in Joshua Tree National Park, California, *in* Keeley, J.E., Baer-Keeley, M., and Fotheringharn, C.J., eds., 2nd interface between ecology and land development in California: U.S. Geological Survey Open-File Report 2000–62, p. 79–85, https://doi.org/10.3133/ofr0062.

MacMahon, J.A., and Wagner, F.H., 1985, The Mojave, Sonoran, and Chihuahuan deserts of North America, *in* Evenari, M., Noy-Meir, I., and Goodall, D.W., eds., Ecosystems of the world 12A—Hot deserts and arid shrublands: New York, Elsevier Press, p. 105–202.

McGaughey, R.J., 2018., Fusion/LDVv 3.8—Software for LIDAR data analysis and visualization: United Stated Department of Agriculture, Forest Service, Pacific Northwest Research Station, accessed at http://forsys.cfr.washington.edu.

Reynolds, M.B.J., DeFalco, L.A., and Esque, T.C., 2012, Short seed longevity, variable germination conditions, and infrequent establishment events provide a narrow window for *Yucca brevifolia* (Agavaceae) recruitment: American Journal of Botany, v. 99, p. 1647–1654, https://doi.org/10.3732/ajb.1200099.

Rowlands, P., 1978, The vegetation dynamics of the Joshua tree (*Yucca brevifolia* Engelm.) in the southwestern United States of America: Riverside, University of California, Ph.D. dissertation. 192 p.

Smith, C.I., Tank, S., Godsoe, W., Levenick, J., Strand, E., Esque, T., and Pellmyr, O., 2011, Comparative phylogeography of a coevolved community—Concerted population expansions in Joshua trees and four yucca moths: PLoS One, v. 6, no. 10, p. e25628, https://doi.org/10.1371/journal.pone.0025628.

Tierra Data, Inc., 2014, Integrated Natural Resources Management Plan, Naval Air Weapons El Centro: El Centro, Calif., 904 p., https://www.cnic.navy.mil/content/dam/cnic/cnrsw/NAVFACSW%20Environmental%20Core/ElCentro_INRMP_signed.pdf.

U.S. Fish and Wildlife Service, 2016, Endangered and Threatened Species: 90-Day Findings on Petition to List the Joshua Tree, November 14, 2016: Federal Register docket number FWS-R8-ES-2016-0088-0003, https://www.regulations.gov/docket?D=FWS-R8-ES-2016-0088.

For more information concerning the research in this report, contact the
Director, Western Ecological Research Center
U.S. Geological Survey
3020 State University Drive East
Sacramento, California 95819
https://www.usgs.gov/centers/werc

Publishing support provided by the U.S. Geological Survey
Science Publishing Network, Sacramento Publishing Service Center

ISSN 2328-0328 (online)
https://doi.org/10.3133/sir20205053